

# UC Riverside

## UC Riverside Previously Published Works

### Title

Efficient label-free chemiluminescent immunosensor based on dual functional cupric oxide nanorods as peroxidase mimics

### Permalink

<https://escholarship.org/uc/item/1q76922r>

### Authors

Li, Juan  
Cao, Yue  
Hinman, Samuel S  
[et al.](#)

### Publication Date

2018-02-01

### DOI

10.1016/j.bios.2017.09.011

Peer reviewed



Published in final edited form as:

*Biosens Bioelectron.* 2018 February 15; 100: 304–311. doi:10.1016/j.bios.2017.09.011.

## Efficient label-free chemiluminescent immunosensor based on dual functional cupric oxide nanorods as peroxidase mimics

Juan Li<sup>a</sup>, Yue Cao<sup>a</sup>, Samuel S. Hinman<sup>b</sup>, Kristy S. McKeating<sup>c</sup>, Yiwen Guan<sup>a</sup>, Xiaoya Hu<sup>a</sup>, Quan Cheng<sup>b,c,\*</sup>, and Zhanjun Yang<sup>a,\*\*</sup>

<sup>a</sup>School of Chemistry and Chemical Engineering, Yangzhou University, Yangzhou 225002, PR China

<sup>b</sup>Environmental Toxicology, University of California, Riverside, CA 92521, United States

<sup>c</sup>Department of Chemistry, University of California, Riverside, CA 92521, United States

### Abstract

Dual-functional cupric oxide nanorods (CuONRs) as peroxidase mimics are proposed for the development of a flow-through, label-free chemiluminescent (CL) immunosensor. Forming the basis of this cost-efficient, label-free immunoassay, CuONRs, synthesized using a simple hydrothermal method, were deposited onto epoxy-activated standard glass slides, followed by immobilization of biotinylated capture antibodies through a streptavidin bridge. The CuONRs possess excellent catalytic activity, along with high stability as a solid support. Antigens could then be introduced to the sensing system, forming large immunocomplexes that prevent CL substrate access to the surface, thereby reducing the CL signal in a concentration dependent fashion. Using carcinoembryonic antigen (CEA) as a model analyte, the proposed label-free immunosensor was able to rapidly determine CEA with a wide linear range of 0.1–60 ng mL<sup>-1</sup> and a low detection limit of 0.05 ng mL<sup>-1</sup>. This nanozyme-based immunosensor is simple, sensitive, cost-efficient, and has the potential to be a very promising platform for fast and efficient biosensing applications.

### Keywords

Dual-functionalization; Cupric oxide nanorods; Immunosensor; Peroxidase mimetics; Chemiluminescence; Carcinoembryonic antigen

## 1. Introduction

Artificial enzymes have gained significant interest in recent years (Bonar-law and Sanders, 1995; Gao et al., 2007; Lin et al., 2014a) due to the numerous intrinsic defects natural enzymes suffer from, which include limited sources, poor stability, and high sensitivity to environmental changes leading to denaturation and inactivation (Shoji and Freund, 2001; Nelson and Cox, 2005; Wei and Wang, 2008). As a result, the design of artificial,

\*Corresponding author at: School of Chemistry and Chemical Engineering, Yangzhou University, Yangzhou 225002, PR China, quan.cheng@ucr.edu (Q. Cheng). \*\*Corresponding author. zjyang@yzu.edu.cn (Z. Yang).



clinical tumor diagnosis and evaluating curative effects (Fu et al., 2006). In this work, a novel and facile label-free CL immunosensor based on dual-functional CuO nanorods (CuONRs) is proposed for the highly sensitive detection of CEA. CuONRs, which were synthesized by a simple hydrothermal method, served not only as a peroxidase mimic to catalyze the CL reaction, but also as a solid support for the immobilization of biomolecules and recognition elements. The construction and design of our nanoparticle-mediated, label-free CL assay is illustrated in Scheme 1. A CuONR-chitosan solution was first coated onto an epoxy-modified glass slide to form a solid CuONRs-chitosan support. Streptavidin was then used to functionalize the composite for highly selective capture of biotinylated antibodies. The immunocomplexes formed on the sensing interface after online incubation are shown to hinder the diffusion of the CL substrate molecules to the CuONR surface. These restrictions effectively inhibit the nanozyme-catalyzed CL reaction, thereby leading to a decrease in CL signal with increasing analyte concentration, without the need for target labeling or enhancement schemes. This research opens a promising avenue for the development of robust and efficient label-free CL immunoassay methods.

## 2. Materials and methods

### 2.1. Chemicals and materials

Biotin-labeled mouse monoclonal CEA antibody (biotinylated anti-CEA,  $2 \mu\text{g mL}^{-1}$ ) and CEA antigen standard solutions ( $0\text{--}75 \text{ ng mL}^{-1}$ ) from a CEA ELISA reagent kit were obtained from CanAg Diagnostics (Beijing, China). The reference CEA electrochemiluminescent (ECL) immunoassay reagent kit was supplied by Roche Diagnostics GmbH (Germany). The clinical serum samples were provided by Jiangsu Institute of Cancer Research. Copper chloride dihydrate ( $\text{CuCl}_2 \cdot 2\text{H}_2\text{O}$ ), anhydrous sodium citrate, sodium hydroxide (NaOH), hydrogen peroxide (30%,  $\text{H}_2\text{O}_2$ ) and Tween-20 were purchased from Sinopharm Chemical Reagent Co. Ltd. (Beijing, China). Bovine serum albumin (BSA), streptavidin, 3-glycidypropyltrimethoxysilane (GPTMS, 98%) and chitosan were purchased from Sigma-Aldrich Chemical Co. (St. Louis, MO). *p*-Iodophenol (PIP) and luminol were obtained from Alfa Aesar Ltd. (China) and Acros (Belgium), respectively. A luminol stock solution (0.01 M) was prepared in 100 mL NaOH (0.1 M). PIP stock solution (0.01 M) was prepared by dissolving 110 mg PIP in 5 mL dimethylsulfoxide and then diluted with water to 50 mL. Prior to use, luminol and PIP stock solutions were mixed and diluted with 0.1 M Tris-HCl buffer (pH 8.5). The final CuONR enzymatic CL substrate concentrations were: 5 mM luminol, 0.6 mM PIP, and 4 mM  $\text{H}_2\text{O}_2$ . Deionized water was used throughout all experiments, and all commercial chemicals were of analytical grade and used as received.

### 2.2. Buffers

Coupling buffer consisted of 0.01 M phosphate buffer solution (PBS, pH 7.4), which was employed for streptavidin and antibody immobilization. Blocking buffer was prepared by adding 1% (w/v) BSA to 0.01 M PBS (BSA, pH 7.4), which was used to block any residual reactive sites on the exposed immunosensor surface. Washing buffer was prepared by spiking 0.05% (v/v) Tween-20 into 0.01 M PBS (PBST, pH 7.4) to minimize nonspecific adsorption.

### 2.3. Instruments

The proposed label-free CL immunosensing platform consisting of a flow cell, flow-injection sampling system, and photomultiplier (PMT) detector is illustrated in Fig. S1 (Supporting information). The flow cell consists of a Teflon cover (length 4.0 cm, width 2.5 cm, height 0.8 cm) with inlet and outlet ports, a silicone rubber spacer (thickness, 2.0 mm), and a transparent plexiglass window (thickness, 0.5 cm). The flow-injection sampling system included the following components: Teflon tubing (i.d., 0.8 mm) and silicone rubber tubing (i.d., 1.0 mm) were used to connect all parts of the flow-through system; a multichannel, bidirectional peristaltic pump was employed to deliver all solutions into the immunosensing system; a multiposition valve, with five inlets and a single outlet, was utilized to introduce different solutions into the flow cell. The flow cell was connected to the flow-through system, and placed on the front of the PMT, which was used to detect CL signals at a working voltage of  $-600$  V. The instrument control and data recording/processing were performed by IFFM software running under Windows XP.

The flow-through CL measurements were taken by an IFFM-E Luminescent Analyzer manufactured by Remex Analytical Instrument Co. Ltd. (Xi'an, China). The reference ECL immunoassay was conducted using a Roche Elecsys 2010 immunoassay analyzer supplied by Roche Diagnostics GmbH. Scanning electron micrographs (SEM) were obtained by a Hitachi S-4800 (Japan) scanning electron microscope (acceleration voltage, 15 kV). Transmission electron micrographs (TEM) were obtained by a Philips Tecnai12 (Holland) electron microscope (acceleration voltage, 120 kV). Extinction spectroscopy measurements were taken using a UV-2550 spectrophotometer supplied by Shimadzu Co. (Japan), and Fourier transform infrared (FT-IR) spectra were collected using a Tensor 27 spectrophotometer from Bruker Co. (Germany). X-ray powder diffractions (XRD) were performed on a D8 Advance X-Ray diffractometer from Bruker Co. (Germany). The static water contact angles were obtained with a Rame-Hart-100 contact angle goniometer using a 20  $\mu$ L droplet of deionized water at 25  $^{\circ}$ C. Electrochemical impedance spectroscopy (EIS) was performed with an Autolab/PGSTAT30 (The Netherlands) in 0.1 M KCl solution containing 5 mM  $\text{K}_3[\text{Fe}(\text{CN})_6]/\text{K}_4[\text{Fe}(\text{CN})_6]$ . The amplitude of the applied sine wave potential was 5 mV, and the frequency range was 0.05–10 kHz at a bias potential of 190 mV.

### 2.4. Preparation of CuONRs

CuONRs were chemically synthesized using a standard hydrothermal method (Zhu and Diao, 2012). 5.0 g  $\text{CuCl}_2 \cdot 2\text{H}_2\text{O}$  and 10.0 g sodium citrate were first dissolved in 160 mL deionized water, and 3.0 g NaOH was added into the solution with continuous stirring for 30 min. Subsequently, the resultant homogenous solution was transferred into a Teflon vessel within a hydrothermal, pressured reactor, which was heated to 180  $^{\circ}$ C for 6 h. After the solution was allowed to cool to room temperature (RT), the obtained precipitate was washed thoroughly with deionized water, followed by ethanol three times. The purified, brown CuONR powder was obtained after drying the final solution at 60  $^{\circ}$ C for 12 h.

### 2.5. Preparation of the label-free immunosensor

A glass slide with 2.1 cm length, 0.4 cm width, and 0.1 cm height was first activated with hydroxyl groups by soaking in piranha solution ( $\text{H}_2\text{SO}_4/30\% \text{H}_2\text{O}_2$ , 7:3 v/v) overnight at

RT. Then, the glass slide was washed thoroughly with deionized water and dried with a stream of nitrogen. Subsequently, the glass slide was soaked in 1% v/v GPTMS toluene solution for 12 h at RT. Following this, the slide was rinsed alternately with toluene and ethanol three times to remove the nonspecifically adsorbed GPTMS, and finally dried with a stream of nitrogen, leaving the glass slide functionalized with epoxy groups (Yang et al., 2013). Two milligrams of CuONRs were dispersed in 1.0 mL deionized water with ultrasonication, which was then mixed with an equal volume of 1.0 wt% chitosan solution under ultrasonication. 20  $\mu\text{L}$  of the resulting CuONR/chitosan solution was deposited on the epoxy-activated glass substrate, and incubated at RT until dry. The epoxy groups on the modified glass substrate react with the free primary amines of chitosan to form a stable, solid CuONRs-chitosan composite membrane, which was used both as the CL sensing interface and as a solid support for further attachments.

Next, 20  $\mu\text{L}$  of 50  $\mu\text{g mL}^{-1}$  streptavidin solution was dropped on the CuONRs-chitosan membrane for 30 min at RT, and stored in a refrigerator at 4 °C overnight (Lin et al., 2004a). After washing several times with PBST, 3.0  $\mu\text{g mL}^{-1}$  biotinylated anti-CEA antibodies were dropped on the streptavidin-functionalized membrane for 3 h at RT, followed by washing several times with PBST and blocking with BSA for 12 h at 4 °C. Finally, the antibody-modified glass slide was inserted into the CL flow cell (Fig. S1, Supporting Information), with an interior volume of *ca.* 80  $\mu\text{L}$  ( $2.1 \times 0.5 \times 0.09$  cm). The prepared immunosensor was stored in 0.01 M PBS (pH 7.4) at 4 °C prior to use.

## 2.6. Flow-through label-free CL immunoassay protocol

A detailed assay procedure of the proposed label-free CL immunosensing system is provided in Scheme 1 and Table S1 (Supporting information). First, 80  $\mu\text{L}$  of a CEA standard solution or serum sample was introduced into the sensing chamber and incubated under zero flow conditions for 25 min at RT. PBST was then injected and used to wash the immunosensor at a flow rate of 1.0  $\text{mL min}^{-1}$ , removing any unbound reagents. Finally, the CL substrate solution (luminol/PIP/ $\text{H}_2\text{O}_2$ , described above) was injected into the chamber, triggering the nanoenzymatic CL reaction while incubated. The CL signals were recorded at a reaction time of 400 s, resulting in a total assay time of 36 min.

## 2.7. Patient specimen collection and safety considerations

According to rules set by the local ethical committee, blood specimens were collected using a standard venipuncture technique and the sera were centrifugally separated from the cells, without hemolysis. The serum samples were then directly assayed with the proposed CL immunosensor and reference method. If necessary, the samples could be stored at 4 °C for up to 48 h or frozen at  $-20$  °C for no more than 2 months. Prior to use, the samples were allowed to reach RT while gently mixing. All handling and processing of clinical samples were performed while wearing appropriate protective equipment, and all tools in contact with patient specimens and immunoreagents were disinfected after use.

### 3. Results and discussion

#### 3.1. Characterization of CuONRs

Enzyme-mimetic CuONRs serve in an essential, dual-functional capacity in the construction of the proposed flow-through, label-free CL immunosensing platform, and were therefore extensively characterized. The morphology of the as-synthesized CuONRs was examined using scanning electron microscopy (SEM) and transmission electron microscopy (TEM). As seen from the SEM (Fig. 1A) and TEM (Fig. S2, Supporting information) images, the CuO particles exhibit distinct nanorod-like morphologies, of which the size ranged from 30 to 90 nm in diameter and 120–300 nm in length. Elemental content and distribution were further examined by energy dispersive X-ray spectroscopy (EDS) (Fig. 1B). The EDS spectrum showed characteristic peaks corresponding to copper and oxygen with an atomic ratio of about 4:5 (Cu/O). The content of oxygen in the prepared product is slightly higher than pure CuO, which may be attributed to sodium citrate adsorbed to the CuONR surfaces, enhancing the colloidal stability of these particles in solution (Zhu et al., 2012).

FT-IR was supplementarily used to confirm the chemical makeup of the CuONRs. As shown in Fig. 1C, the FT-IR spectrum of CuONRs exhibited three clear absorption peaks at 583, 551 and 494  $\text{cm}^{-1}$ , which matched well with the characteristic absorption peaks of pure Cu(II)-O (Zhang et al., 2006). In addition, the molecular vibration band of Cu<sub>2</sub>(I)-O at 610  $\text{cm}^{-1}$  was not observed from the FT-IR spectrum of the CuONRs synthesized here, suggesting pure CuO with no reaction byproducts. XRD was also used to characterize the crystal structure of the CuONRs. As shown in Fig. 1D, the products only displayed the XRD peak characteristic of CuO (JCPDS card no. 48–1548), which further confirmed that only the single monoclinic phase of CuONRs was produced. Taken together, these results indicate that the hydrothermal method used in this work is a simple and highly effective way to produce pure CuONRs in a consistent fashion.

#### 3.2. Peroxidase-like activity of CuONRs

The peroxidase mimicking activity of the as-prepared CuONRs was evaluated by the catalytic oxidation of TMB in the presence of H<sub>2</sub>O<sub>2</sub> (shown in Fig. 2A). The catalytic process was assessed by measuring the absorbance of the substrate solution at 652 nm, the characteristic absorption wavelength of the catalyzed TMB product, over time using UV–vis spectroscopy. Upon mixing of the CuONRs and TMB-H<sub>2</sub>O<sub>2</sub> substrates, the solution turned from colorless to blue (inset photograph **2**, Fig. 2A), characteristic of the charge transfer complex of TMB, and the absorbance at 652 nm rapidly increased over a reaction time of 800 s (Curve **a**, Fig. 2A). Conversely, the TMB-H<sub>2</sub>O<sub>2</sub> solution without CuONRs remained colorless (inset photograph **1**, Fig. 2A), and the absorbance at 652 nm displayed no obvious change (Curve **b**, Fig. 2A). However, the observed catalytic activity has previously been shown to be caused by copper ions leached from the CuONRs, rather than by nanoenzymatic catalysis of CuO at the particle surface (Chen et al., 2012). To rule out this possibility, a “leaching solution” was used to test the reaction under the same experimental conditions. The leaching solution was prepared by incubating the CuONRs with standard acetate buffer solution (pH 3.0) for 10 min at RT, followed by separation through centrifugation (Gao et al., 2007). As can be seen from Curve **c** (Fig. 2A), the leaching solution, containing only

copper ions, exhibited no catalytic activity, indicating that the observed peroxidase mimicking activity came entirely from the CuONRs. These results demonstrate that the prepared CuONRs possess intrinsic nanozyme characteristics, which can be used within standard assays that incorporate colorimetric reporters.

### 3.3. Nanozyme-mediated, label-free CL immunosensor feasibility

In order to explore the feasibility and mechanism behind the proposed label-free immunosensing method, the CL response from various systems were examined by incubating several different concentrations of CEA (0, 30 and 75 ng mL<sup>-1</sup>, shown in Fig. 2B) on the sensor. In all further experiments, the CL generating substrate used consisted of 5 mM luminol, 0.6 mM PIP, and 4 mM H<sub>2</sub>O<sub>2</sub>, and will be denoted as CS. When the CS was exposed to anti-CEA alone, a particularly low CL response was observed, which did not display any concentration-dependent change after incubation with CEA. When the CS was exposed to CuONRs alone, a very high CL response was generated, indicating that the prepared CuONRs have an intrinsic enzymatic activity towards the CL substrate, in addition to TMB. However, there was still no change in CL intensity when the concentration CEA was varied within this system. Alternatively, when the CS was exposed to both CuONRs and anti-CEA, not only was a high CL response observed, but also a concentration-dependent decrease in CL intensity after incubation with 30 and 75 ng mL<sup>-1</sup> CEA. It can be inferred that the formed immunocomplex efficiently blocks the CL substrate from accessing the CuONR surface, inhibiting the enzymemimetic CL reaction, and thereby decreasing the CL response. Consequently, the proposed CuONR-based label-free CL immunoassay strategy is shown to be feasible for the detection of tumor biomarkers.

### 3.4. Characterizations of the fabricated label-free immunosensors

The efficient immobilization of capture antibodies on the CuONRs-chitosan interface for binding a target antigen is a key factor in the success of this label-free sensing strategy. Therefore, it was necessary to investigate the fabrication process for the proposed immunosensor. SEM was first utilized to examine the surface morphology of the CuONRs-chitosan membrane and the immunosensor. Fig. 3A(a) shows the SEM image of the CuONRs-chitosan composite formed on an epoxy-activated glass slide. As exhibited in this image, the CuONRs were evenly embedded within the chitosan film. After the composite membrane was functionalized with streptavidin molecules, protein aggregates were clearly observed on the surface (Fig. 3A (b)). With further immobilization of biotinylated anti-CEA antibodies on the membrane (Fig. 3A (c)), a different surface morphology emerged, with almost complete coverage of antibodies on the CuONRs-chitosan composite, thus providing evidence that the formed CEA immunocomplex could effectively block the diffusion of CL substrate to CuONRs mimetics.

Static water contact angle measurements were employed to study the hydrophilicity of the interface during the fabrication process of the immunosensor. Fig. S3 (Supporting Information) shows the contact angle images of bare (a), piranha-treated (b), and GPTMS-silanized (c). Fig. 3B shows the contact angle images of CuONRs-chitosan-modified (a), streptavidin/CuONRs-chitosan-modified (b) and anti-CEA antibody-modified (c) glass substrates. Their corresponding contact angle values were 45.5°, 33.7°, 51.2°, 61.5°, 21.2°

and 10.2°, respectively. The piranha-treated glass substrate displayed a smaller contact angle compared to the bare glass substrate, indicating the successful activation with abundant hydroxyl groups on the surface. For the GPTMS-silanized glass slide, a higher contact angle was observed due to the presence of epoxy groups functionalized to the glass slide. The CuONRs-chitosan composite exhibited an even higher contact angle, suggesting the formation of the stable composite membrane. After the membrane was functionalized with streptavidin, the contact angle of the streptavidin/CuONRs-chitosan-modified substrate greatly decreased, indicating greater hydrophilicity, which provided a favorable microenvironment for retaining bioactivity of the loaded antibodies. The contact angle of the biotinylated anti-CEA antibody immobilized glass substrate exhibited the smallest value, demonstrating that the capture antibodies were successfully immobilized at the sensing interface.

### 3.5. Optimization of the experimental conditions

Reagent incubation times are a key factor in dictating the overall assay speed, and were optimized using 30 ng mL<sup>-1</sup> CEA standard solution. CL measurements were taken 400 s after CS (80 μL) addition to the antigen-treated surface, which offered a compromise between measurement speed and sensitivity (Fig. S5A). In investigating target incubation (Fig. S5B), the CL response decreased rapidly with increasing CEA incubation time, and tended to level off after 25 min, indicating that the immunocomplex formed on the interface had almost reached saturation. Thus, 25 min was chosen as the optimal incubation time for the proposed label-free immunoassay, which is significantly shorter than traditional multi-well plate-based ELISA (Zhao et al., 2004) and other labeled immunoassay methods, which may range from hours to days (Kimura et al., 1996; Hou et al., 2012; Li et al., 2017). This relatively short assay time is attributed to the following reasons: i) the proposed label-free strategy only requires a one-step incubation once the sensor is constructed, with online washing steps; ii) the CuONR supports have a large specific surface area, which was advantageous toward formation of the CS-blocking immunocomplex; iii) the streptavidin-functionalized composite interface could produce oriented immobilization of biotinylated antibodies, which would be favorable for mass transport of antigens. As demonstrated, the proposed immunosensing platform is fast, simple and cost-efficient.

### 3.6. Analytical performance

The capability of this assay design for the quantitation of CEA was studied under the optimal conditions determined in the previous section. As shown in Fig. 3C, CL intensity rapidly decreased with the increasing concentration of CEA antigen, and a very wide linear range from 0.1 to 60 ng mL<sup>-1</sup> for CEA antigen was obtained from the calibration curve (> 3 orders of magnitude), which overall exhibited excellent linearity ( $R^2 = 0.9980$ ). The linear regression equation was  $I_{CL} = 19047.36 - 176.18 C$  ( $I_{CL}$  represents CL intensity, and  $C$  is the concentration of CEA antigen, ng mL<sup>-1</sup>) with a correlation coefficient of 0.9980. The detection limit of the label-free CL immunoassay was evaluated to be 0.05 ng mL<sup>-1</sup> (S/N = 3). A comparison of assay performance between our method and label CL immunoassay as well as other immunoassay methods were listed Table 1. As seen from Table 1, the CuONRs mimic-based label-free method is more sensitive, rapid, simple, and cheap compared to the previous methods. Since the value of CEA in healthy patients is 5 ng mL<sup>-1</sup>, the sensitivity of

the proposed label-free CL immunoassay method was sufficient for practical applications. The proposed use of CuONRs can be prospective for the development of next-generation diagnostic devices (Vashist et al., 2015; Vashist and Luong, 2016).

### 3.7. Specificity, reproducibility and storage stability

To evaluate the specificity of the proposed label CL immunosensor, three different cancer biomarkers, CEA, AFP, and CA125, along with two negative controls, IgG and BSA, were analyzed. As expected, the CL intensity of the system greatly decreased after the incubation of CEA, but showed no obvious changes for the other biomolecules (Fig. 4A). These results indicate that this immunosensor exhibits relatively specific recognition for CEA in the presence of other interferents.

The reproducibility of the label-free CL immunosensor was evaluated by intra- and inter-assay coefficients of variation (CVs). In this experiment, the intra- and inter-assay CVs based on five separate measurements were examined by incubating 30 ng mL<sup>-1</sup> CEA antigen. The values for intra- and inter-assay CVs were 5.6% and 8.7%, respectively, demonstrating acceptable reproducibility of the proposed immunosensor.

The storage stability of the fabricated label-free CL immunosensor was evaluated by examining the CL response over 30 days of storage time (Fig. 4B). The immunosensors were stored in 0.01 M pH 7.4 PBS at 4 °C, and CL measurements were performed by incubating with 30 ng mL<sup>-1</sup> CEA at an interval of every 5–10 days. It can be seen that the CL response of the immunosensor only decreased by 4.9% over thirty days of storage, indicating acceptable storage stability of the proposed label-free CL immunosensor.

### 3.8. Analytical applications

In order to explore reliability and potential application of the proposed nanozyme-based CL immunosensing platform, CEA levels in human serum samples (provided by Jiangsu Institute of Cancer Research) were tested. When the level of serum tumor marker was beyond the calibration range of the label-free immunosensor, the serum samples were diluted appropriately with 0.01 M PBS (pH 7.4). The results were in good agreement with those obtained using an ECL immunoassay, which was conducted by Jiangsu Institute of Cancer Research. As shown in Table S3, the relative errors of CEA concentrations obtained by the proposed method and the reference method were less than 7.5%, which indicated that the proposed immunosensing platform could be used in the determination of CEA concentrations in clinical practical samples.

## 4. Conclusion

In this study, we developed a novel and cost-efficient, nanozyme-based CL immunosensor for highly sensitive detection of tumor markers based on dual functional CuONRs. The effective CuONRs were synthesized by a facile hydrothermal method with high catalytic ability and stability, which acted as both a peroxidase-mimicking nanozyme and a solid support. The label-free immunosensor could be simply fabricated by immobilizing capture antibodies onto the biofunctionalized CuONRs-chitosan composite through biotin-avidin interactions. The resultant CuONRs and immunosensor were well characterized by TEM,

SEM, static contact angles, EIS, and FT-IR. This immunoassay method is simple, low-cost, and can be used for rapid determination of tumor markers based on the linear decrease of CL intensity with the increasing concentration of antigen. In addition, the constructed immunoassay exhibited high sensitivity, excellent specificity, and acceptable reproducibility and accuracy. This work provides a novel and alternative avenue to construct cost-efficient CL immunosensing platforms for tumor diagnostics.

## Supplementary Material

Refer to Web version on PubMed Central for supplementary material.

## Acknowledgments

The financial support for this work was provided by National Natural Science Foundation of China (no. 21475116, 21575125, and 21575124), Qinglan Project of Jiangsu Province for Zhanjun Yang, Priority Academic Program Development of Jiangsu Higher Education Institution (PAPD), the Six Talent Peaks Project of Jiangsu Province for Juan Li, High-end talent support program of Yangzhou University, and the US National Science Foundation (CHE-1413449 to Q.C.). S.S.H. was supported by a University of California, Riverside (UCR) Dissertation Year Fellowship, and an NIEHS T32 training grant (T32 ES018827). In addition, many thanks are given to the Testing Center of Yangzhou University for all of the characterizations that were performed.

## Appendix A. Supplementary material

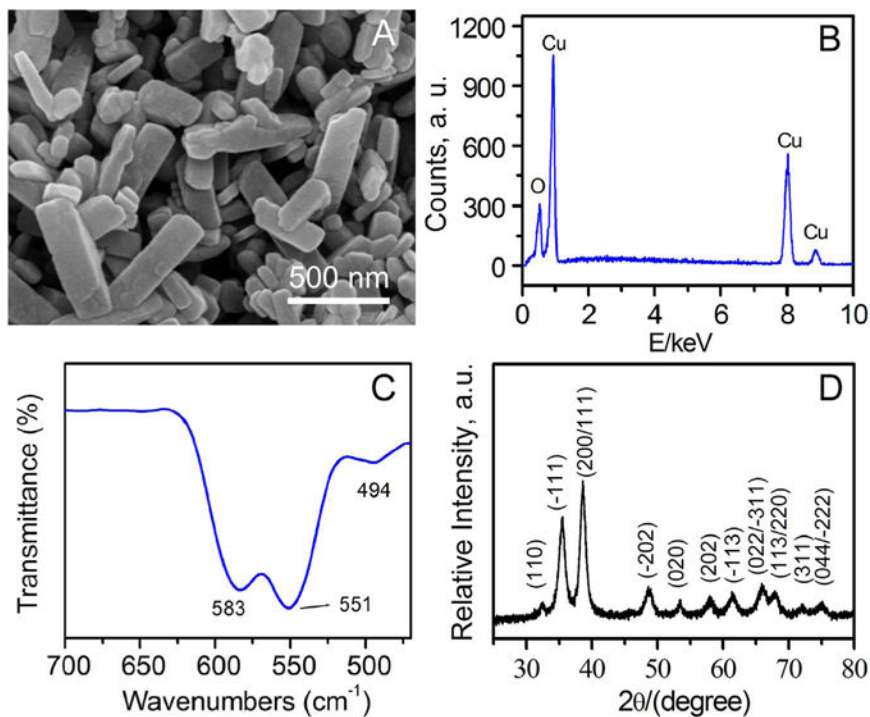
Supplementary data associated with this article can be found in the online version at <http://dx.doi.org/10.1016/j.bios.2017.09.011>.

## References

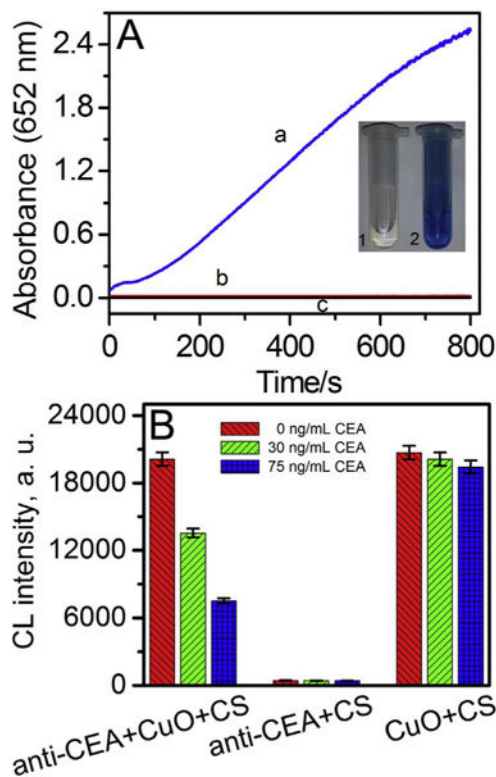
- Adam W, Kazakov DV, Kazakov VP. *Chem Rev.* 2005; 105:3371–3387. [PubMed: 16159156]
- André R, Natálio F, Humanes M, Leppin J, Heinze K, Wever R, Schröder HC, Müller WEG, Tremel W. *Adv Funct Mater.* 2011; 21:501–509.
- Asati A, Santra S, Kaitanis C, Nath S, Perez JM. *Angew Chem Int Ed.* 2009; 48:2308–2312.
- Bonar-law RP, Sanders JKM. *J Am Chem Soc.* 1995; 117:259–271.
- Chen W, Chen J, Feng YB, Hong L, Chen QY, Wu LF, Lin XH, Xia XH. *Analyst.* 2012; 137:1706–1712. [PubMed: 22349179]
- Chen FM, Mao SF, Zeng HL, Xue SH, Yang JM, Nakajima H, Lin JM, Uchiyama K. *Anal Chem.* 2013; 85:7413–7418. [PubMed: 23815610]
- Date Y, Aota A, Sasaki K, Namiki Y, Matsumoto N, Watanabe Y, Ohmura N, Matsue T. *Anal Chem.* 2014; 86:2989–2996. [PubMed: 24528234]
- Dong YL, Zhang HG, Rahman ZU, Su L, Chen XJ, Hu J, Chen XG. *Nanoscale.* 2012; 4:3969–3976. [PubMed: 22627993]
- Fu ZF, Liu H, Ju HX. *Anal Chem.* 2006; 78:6999–7005. [PubMed: 17007526]
- Fu ZF, Yang ZJ, Tang JH, Liu H, Yan F. *Anal Chem.* 2007; 79:7376–7382. [PubMed: 17713968]
- Gao J, Guo ZK, Su FJ, Gao L, Pang XH, Gao W, Du B, Wei Q. *Biosens Bioelectron.* 2015; 63:465–471. [PubMed: 25129508]
- Gao LZ, Zhuang J, Nie L, Zhang JB, Zhang Y, Gu N, Wang TH, Feng J, Yang DL, Perrett S, Yan XY. *Nat Nanotechnol.* 2007; 2:577–583. [PubMed: 18654371]
- Gao ZQ, Xu MD, Hou L, Chen GN, Tang DP. *Anal Chim Acta.* 2013; 776:79–86. [PubMed: 23601285]
- Genfa Z, Dasgupta PK. *Anal Chem.* 1992; 64:517–522. [PubMed: 1575321]
- Guan GJ, Yang L, Mei QS, Zhang K, Zhang ZP, Han MY. *Anal Chem.* 2012; 84:9492–9497. [PubMed: 23025448]

- Hong L, Liu AL, Li GW, Chen W, Lin XH. *Biosens Bioelectron.* 2013; 43:1–5. [PubMed: 23274189]
- Hou JY, Liu TC, Lin GF, Li ZX, Zou LP, Li M, Wu YS. *Anal Chim Acta.* 2012; 734:93–98. [PubMed: 22704477]
- Hu LZ, Yuan YL, Zhang L, Zhao JM, Majeed S, Xu GB. *Anal Chim Acta.* 2013; 762:83–86. [PubMed: 23327949]
- Jiang X, Sun CJ, Guo Y, Nie GJ, Xu L. *Biosens Bioelectron.* 2015; 64:165–170. [PubMed: 25218100]
- Kimura H, Matsuzawa S, Tu CY, Kitamori T, Sawada T. *Anal Chem.* 1996; 68:3063–3067. [PubMed: 8794934]
- Li NL, Jia LP, Ma RN, Jia WL, Lu YY, Shi SS, Wang HS. *Biosens Bioelectron.* 2017; 89:453–460. [PubMed: 27151437]
- Lin JH, Yan F, Hu XY, Ju HX. *J Immunol Methods.* 2004a; 291:165–174. [PubMed: 15345314]
- Lin JH, Yan F, Ju HX. *Clin Chim Acta.* 2004b; 341:109–115. [PubMed: 14967165]
- Lin XX, Chen QS, Liu W, Li HF, Lin JM. *Biosens Bioelectron.* 2014b; 56:71–76. [PubMed: 24469539]
- Lin YH, Ren JS, Qu XG. *Acc Chem Res.* 2014a; 47:1097–1105. [PubMed: 24437921]
- Lin TR, Zhong LS, Song ZP, Guo LQ, Wu HY, Guo QQ, Chen Y, Fu FF, Chen GN. *Biosens Bioelectron.* 2014c; 62:302–307. [PubMed: 25032681]
- Liu ZH, Cai RX, Mao LY, Huang HP, Ma WH. *Analyst.* 1999; 124(38):173–176.
- Liu JT, Qu SX, Luo JP, Wang B, Cai XX. *Chin J Electron.* 2017; 26:152–155.
- Liu YM, Mei L, Liu LJ, Peng LF, Chen YH, Rei SW. *Anal Chem.* 2011; 83:1137–1143. [PubMed: 21218847]
- Luong JHT, Vashist SK. *Biosens Bioelectron.* 2017; 89:293–304. [PubMed: 26620098]
- McKeating KM, Sloan-Dennison S, Graham D, Faulds K. *Analyst.* 2013; 138:6347–6353. [PubMed: 24022024]
- Nelson DL, , Cox MM. *Lehninger Principles of Biochemistry* 4th. W. H. Freeman & Co Ltd.; New York: 2005 Chapter 6
- Okuno J, Maehashi K, Kerman K, Takamura Y, Matsumoto K, Tamiya E. *Biosens Bioelectron.* 2007; 22:2377–2381. [PubMed: 17110096]
- Pang XH, Li JX, Zhao YB, Wu D, Zhang Y, Du B, Ma HM, Wei Q. *ACS Appl Mater Interfaces.* 2015; 7:19260–19267. [PubMed: 26271682]
- Qi YY, Li BX. *Chem Eur J.* 2011; 17:1642–1648. [PubMed: 21268167]
- Shi WB, Zhang XD, He SH, Huang YM. *Chem Commun.* 2011; 47:10785–10787.
- Shoji E, Freund MS. *J Am Chem Soc.* 2001; 123:3383–3384. [PubMed: 11457081]
- Souza TTL, Moraes ML, Ferreira M. *Sens Actuators, B.* 2013; 178:101–106.
- Tang DY, Xia BY. *Microchim Acta.* 2008; 163:41–48.
- Tang DP, Zhang B, Tang J, Hou L, Chen GN. *Anal Chem.* 2013; 85:6958–6966. [PubMed: 23789727]
- Triantis TM, Papadopoulos K, Yannakopoulou E, Dimotikali D, Hrbá J, Zbo il R. *Chem Eng J.* 2008; 144:483–488.
- Vashist SK, Luong JHT. *Biotechnol Adv.* 2016; 34:137–138. [PubMed: 27071536]
- Vashist SK, Luppá PB, Yeo LY, Ozcan A, Luong JHT. *Trends Biotechnol.* 2015; 33:692–705. [PubMed: 26463722]
- Wang XH, Qu KG, Xu BL, Ren JS, Qu XG. *Nano Res.* 2011; 4:908–920.
- Wei H, Wang EK. *Anal Chem.* 2008; 80:2250–2254. [PubMed: 18290671]
- Wei W, Zhang CY, Qian J, Liu SQ. *Anal Bioanal Chem.* 2011; 401:3269–3274. [PubMed: 21928078]
- Xu J, Wu J, Zong C, Ju HX, Yan F. *Anal Chem.* 2013; 85:3374–3379. [PubMed: 23427829]
- Xu YS, Zhang XP, Luan CX, Wang H, Chen BA, Zhao YJ. *Biosens Bioelectron.* 2017; 87:264–270. [PubMed: 27567252]
- Yang ZJ, Cao Y, Li J, Wang JT, Du D, Hu XY, Lin YH. *Chem Commun.* 2015; 51:14443–14446.
- Yang ZJ, Lan QC, Li J, Wu JJ, Tang Y, Hu XY. *Biosens Bioelectron.* 2017; 89:312–318. [PubMed: 27650709]
- Yang ZJ, Liu H, Zong C, Yan F, Ju HX. *Anal Chem.* 2009; 81:5484–5489. [PubMed: 19499927]

- Yang ZJ, Shen J, Li J, Zhu J, Hu XY. *Anal Chim Acta*. 2013; 774:85–91. [PubMed: 23567121]
- Zhang YC, Tang JY, Wang GL, Zhang M, Hu XY. *J Cryst Growth*. 2006; 294:278–282.
- Zhang L, Yang F, Cai JY, Yang PH, Liang ZH. *Biosens Bioelectron*. 2014; 56:271–277. [PubMed: 24514079]
- Zhao Y, Huang YC, Zhu H, Zhu QQ, Xia YS. *J Am Chem Soc*. 2016; 138:16645–16654. [PubMed: 27983807]
- Zhao LX, Sun L, Chu XG. *TRAC Trends Anal Chem*. 2009b; 28:404–415.
- Zhao LS, Xu SY, Fjaertoft G, Pauksen K, Håkansson L, Venge P. *J Immunol Methods*. 2004; 293:207–214. [PubMed: 15541289]
- Zhao YJ, Zhao XW, Hu J, Xu M, Zhao WJ, Sun LG, Zhu C, Xu H, Gu ZZ. *Adv Mater*. 2009a; 21:569–572. [PubMed: 21161983]
- Zhu MY, Diao GW. *Catal Sci Technol*. 2012; 2:82–84.
- Zou QJ, Kegel LL, Booksh KS. *Anal Chem*. 2015; 87:2488–2494. [PubMed: 25526646]

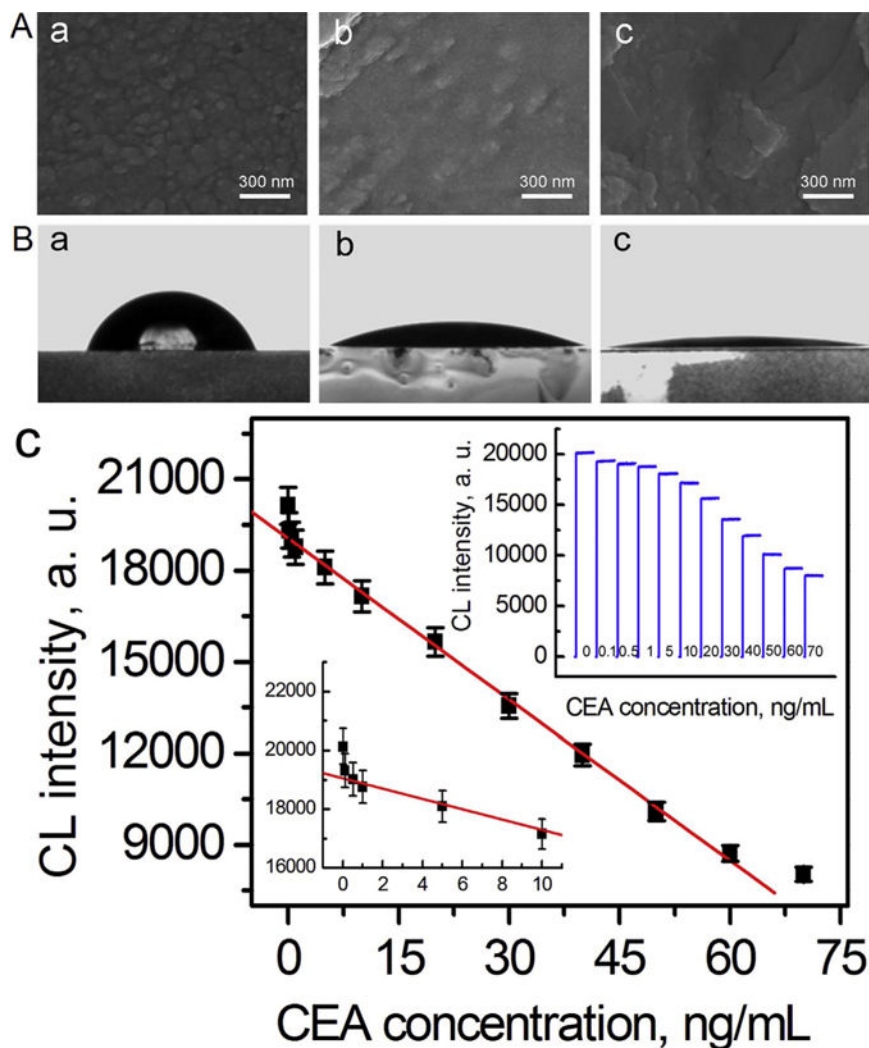


**Fig. 1.** SEM image (A), EDS spectra (B), FT-IR spectra (C) and XRD spectra (D) of the as-synthesized CuONRs.

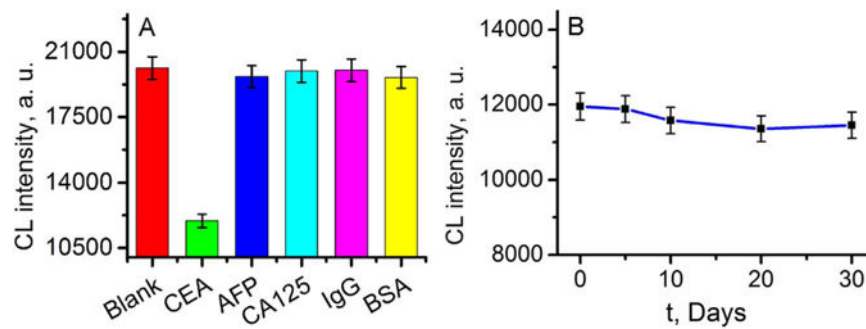


**Fig. 2.**

(A) UV-vis spectra of the TMB (1.0 mM)/H<sub>2</sub>O<sub>2</sub> (100 mM) solution (a), TMB(1.0 mM)/H<sub>2</sub>O<sub>2</sub>(100 mM)/CuONRs (100 μg mL<sup>-1</sup>) solution (b), and TMB(1.0 mM)/H<sub>2</sub>O<sub>2</sub>(100 mM)/leaching solution (c). Inserted photographs: the TMB/H<sub>2</sub>O<sub>2</sub> solution (1) and TMB/H<sub>2</sub>O<sub>2</sub>/CuONRs solution (2), and (B) feasibility of the proposed nanozyme-based label-free CL immunosensing platform. Three systems were incubated with 0, 30 and 75 ng mL<sup>-1</sup> of CEA antigen and the CL signal observed. (PMT: -600 V; n = 5 for each point; incubation time: 25 min; CL reaction time: 400 s).

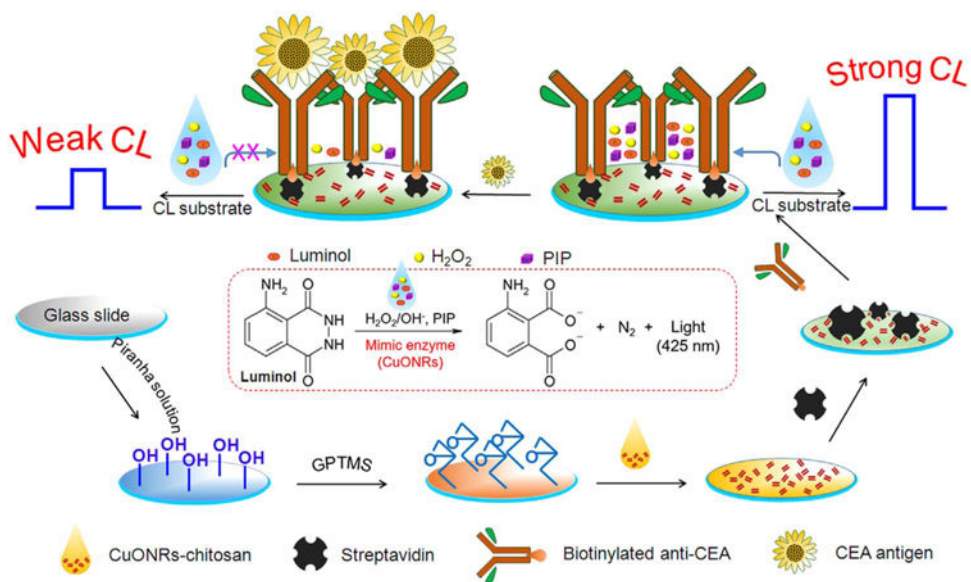


**Fig. 3.** (A) SEM images of the CuONRs-chitosan (a), streptavidin/CuONRs-chitosan (b), and biotinylated anti-CEA/streptavidin/CuONRs-chitosan (c) modified glass slides, (B) the contact angle values of CuONRs-chitosan-modified (a), streptavidin/CuONRs-chitosan-modified (b) and anti-CEA antibody-modified (c) glass slides, AND (C) calibration curve for the label-free CL immunoassay ( $n = 5$  for each data point). Inserts: dose-response curve for CEA (top right), and the enlargement of low-concentration section in the calibration curve (bottom left).



**Fig. 4.**

(A) CL responses of the proposed nanozyme-based label-free CL immunosensor from 0 ng mL<sup>-1</sup> CEA, 30 ng mL<sup>-1</sup> CEA, 30 ng mL<sup>-1</sup> AFP, 30 ng mL<sup>-1</sup> CA125, 100 ng mL<sup>-1</sup> IgG, and 100 ng mL<sup>-1</sup> BSA, and (B) CL responses of the label-free CL immunosensor after storage of the surface for 0 d, 5 d, 10 d, 20 d and 30 d using a CEA concentration of 30 ng mL<sup>-1</sup> (n = 5 for each point).

**Scheme 1.**

Schematic illustration of the proposed CuONR platform for the nanoenzymatic-based label-free detection of CEA.

**Table 1**

Comparison between the proposed label-free CL immunoassay and conventional label immunoassay for detection of CEA.

Immunoassay method	Incubation time (min)	Linear range (ng mL <sup>-1</sup> )	Detect limit (ng mL <sup>-1</sup> )	Reference
Label-free CLIA	25	0.1–60	0.05	This work
HRP-labeled sandwich CLIA	40	1.0–60	0.6	Yang et al. (2009)
HRP-labeled sandwich CLIA	40	1.0–70	0.65	Fu et al. (2007)
HRP-labeled noncompetitive CLIA	25	1.0–25	0.5	Lin et al. (2004b)
HRP-labeled sandwich CLIA	–	1–1000	1.0	Liu et al. (2017)
ALP-labeled sandwich CLIA	60	0.5–80	0.41	Wei et al. (2011)
HRP-labeled competitive ECIA	35	1.0–55	0.13	Tang and Xia (2008)
HRP-labeled sandwich ECIA	30	0.02–12	0.01	Yang et al. (2017)
Eu <sup>3+</sup> -labeled sandwich TRFIA	30	1–1000	0.5	Hou et al. (2012)
HRP-labeled sandwich ELISA	120	0.25–75	0.25	CanAg ELISA Kit
Ru(bpy) <sub>3</sub> <sup>2+</sup> -labeled sandwich ECLIA	–	0.2–1000	–	Roche Diagnostics

CLIA: CL immunoassay.

ALP: alkaline phosphatase.

ECIA: electrochemical immunoassay.

TRFIA: time-resolved fluoroimmunoassay.

ELISA: enzyme-linked immunosorbent assay.

ECLIA: electrochemiluminescent immunoassay.